SUMMER SCHOOL ON THE FUNDAMENTALS OF NEUTRON SCATTERING
NIST CENTER FOR NEUTRON RESEARCH
JUNE 19-23, 2017

Methyl Group Dynamics in Fluorotoluene

HFBS Team: Timothy Prisk, Madhusudan Tyagi, and Jacob Tarver

In this experiment, we will use high-resolution, inelastic neutron scattering to examine methyl group rotations in 4F-toluene. The goal of this hands-on measurement is to gain an understanding and appreciation of neutron backscattering spectroscopy, as well as gain practical experience in collecting, analyzing, and interpreting a set of this data.

1. INTRODUCTION

Quasi-elastic and inelastic neutron scattering techniques provide experimentalists direct probes of the atomic-scale dynamics of materials[CL15]. These methods are especially sensitive to the motion of hydrogen atoms, as the incoherent scattering cross section of hydrogen is very large compared to other nuclei. An important application of neutron backscattering is the field of chemical spectroscopy, including the study of methyl group rotations[Pre81, PH97, Dim03].

In the solid state, methyl groups act as rigid rotors under the influence of an external orientational potential that hinders their movement. That is, the three hydrogen atoms of the methyl group act co-operatively, as a single degree of freedom, rotating about the axis of symmetry of the whole pyramid. There are three distinctive types of motion, each of which can be studied using neutron scattering techniques: libration, stochastic reorientation, and rotational tunneling. The first type of motion is analogous to a classical torsional pendulum and so consists of fast, small amplitude oscillations about the potential minimum. The second type of motion is thermally activated, rotational jump diffusion. Finally, rotational tunneling is a quantum-mechanical phenomenon occurring at low temperatures whereby the methyl

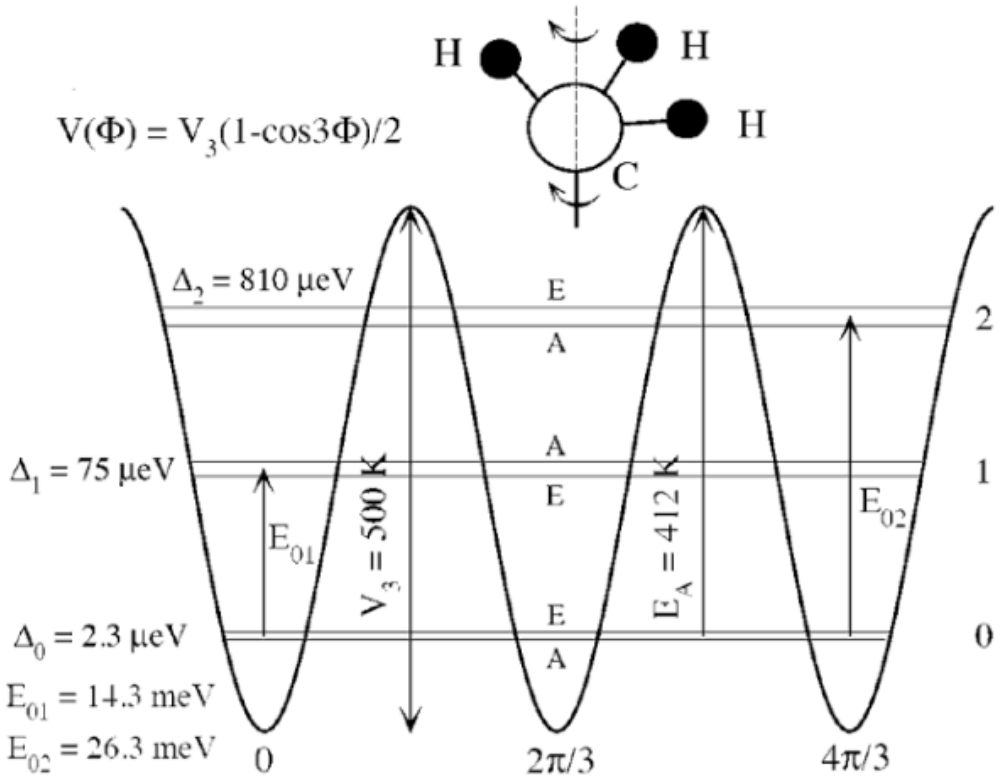

Figure 1.1: The energy levels of a hindered methyl rotor in a three-fold orientational barrier of strength $V_3 = 43.1$ meV are shown[CL15]. The transitions from the librational ground state to the first and second librational excited states are E_{01} and E_{02}, respectively. Each librational state n_{lib} is split between the A and E sublevels with spacing Δ_n by quantum-mechanical tunneling.

group rotates through the potential barrier, despite classically lacking sufficient kinetic energy to do so.

A generic energy level diagram for a methyl group in a three-fold orientational potential is shown in Figure 1.1. The librational mode may be described as an (anharmonic) oscillator with quantum number n_{LIB}. The level spacing between the ground state and first excited state of the oscillator is E_{01}. Rotational tunneling of the methyl group through the orientational barrier produces a fine splitting of these oscillator levels, where Δ_0 is the splitting of the librational ground state where $n_{\text{LIB}} = 0$. The transitions between librational energy levels is typically on the order of tens of meV whereas tunnel splitting of the librational states may fall in the range of 1 μeV to 100 μeV, depending upon the strength of the potential.

One may define a set of pocket states for the methyl group where the labeled hydrogen atoms are each localized near the minima of the three-fold potential. However, these pocket states are not energy eigenstates of the methyl group and so these pocket states evolve with

time, $|123\rangle \rightarrow |231\rangle \rightarrow |312\rangle \rightarrow |123\rangle$,at the tunneling frequency $\omega_{\text{tunnel}} = \Delta_0/\hbar$. The energy eigenstates of the methyl group may be expressed as linear superpositions of these pocket states. If the rotational wavefunction of the methyl group is a symmetric combination of the pocket states, then it is said to belong to the A singlet; if the rotational wavefunction is an antisymmetric combination of the pocket states, then it is said to belong to the E doublet. (These states are named for the irreducible representations of the point group C_3.) The tunnel splitting Δ_n is the transition energy between the A singlet and the degenerate E doublet for a given oscillator level n_{lib}.

In this summer school experiment, we will use neutron backscattering to study methyl group tunneling in crystalline 4-fluorotoluene [$C_6H_4FCH_3$][SMT$^+$62, PHLMw90]. As we will see, the observed tunnel splitting is a sensitive measure of the orientational potential barrier. So, we will be able to estimate the depth of the potential well and predict the excitation energy of the librational mode from our neutron backscattering data.

2. Why Use Neutron Backscattering?

When planning a neutron scattering experiment, one should consider whether a given spectrometer is appropriate for carrying out the study. The High Flux Backscattering Spectrometer (HFBS) is well-suited to the study of methyl group rotations because of the length and time scales probed by the instrument, respectively. The momentum $\hbar Q$ and energy $\hbar\omega$ transfer are inversely proportional to the length and time scales under observation. HFBS spans a dynamic range of $0.25\ \text{Å}^{-1} \leq Q \leq 1.75\ \text{Å}^{-1}$ and $-36\ \mu\text{eV} \leq E \leq +36\ \mu\text{eV}$. This corresponds to length scales between 25 Å and 3.6 Å and time scales between 10 ns and 0.1 ns. Methyl group rotations occur along a circumference that is approximately 6.5 Å and at frequencies on the order of GHz, for 'intermediate' barrier strengths.

A second reason for using inelastic neutron scattering to study methyl group rotations is that the interaction of a neutron with a hydrogen atom is spin-dependent. A methyl group is composed of three identical fermions, so its combined rotational and nuclear spin wavefunction must be antisymmetric upon an exchange of the hydrogen atoms. Since a 120° rotation of the methyl group is a cyclic permutation of the hydrogen atoms, a change in its rotational state requires a change in its nuclear spin state. Since neutrons couple directly to the nuclear spin of hydrogen atoms, both the rotational and spin states of the methyl group can change during an inelastic neutron scattering event.

3. What will we do in this experiment?

4-fluorotoluene is a weak glass-forming liquid available commercially. Our sample was purchased from Sigma-Aldrich and will be used in our experiment as prepared by the manufacturer. We loaded approximately 600 μL of 4-fluorotoluene into an aluminum sample can with a 0.1 mm annulus. The sample can was sealed with indium under an ambient atmosphere.

The sample geometry was chosen to minimize the amount of *multiple scattering*. In an ideal neutron scattering measurement, we would like for the neutron to scattering once within the sample before reaching the detector. In practice, neutrons can undergo several scattering

events within the sample and/or be absorbed by the sample. The number of events increases with the thickness of the sample illuminated by the beam. One often used rule-of-thumb is to select the sample geometry so that 90% of the incident neutrons are transmitted in the forward direction. This is often a good compromise between signal and the effects of multiple scattering. Such as a sample is informally referred to as a *10% scatterer*.

For our sample, $C_6H_4FCH_3$, the macroscopic scattering cross sections are: $\Sigma_{inc} = 3.07\ cm^{-1}$, $\Sigma_{coh} = 0.30\ cm^{-1}$; and $\Sigma_{abs} = 0.01\ cm^{-1}$. The incoherent scattering from hydrogen makes largest contribution to the total macroscopic cross section Σ_{tot}, and so our measurements are primarily sensitive to the self-correlation function of the hydrogen atoms. The probability S of scattering from an annulus of thickness t is: $S = (\Sigma_{scatt}/\Sigma_{tot})\left(1 - \exp(-\pi\Sigma_{tot}\, t)\right)$. For our sample, $S = 0.1$. The DAVE software has a planning tool for estimating the macroscopic scattering cross section for a sample of known chemical composition[AKQ+09].

Question: How many times does the beam go through the sample before reaching the detectors?

The answer to this question can have important consequences for your experiment. If the beam pases through the sample twice (for instance) and the sample has an appreciable neutron absorption cross section, then the intensity at the detectors will be lower than if the beam had only passed once through the sample. Additionally, a beam which passes twice through a strongly scattering sample can produce an energy-dependent background. For more details on these points, see the appendices.

The sample will be placed in a top loading closed-cycle refrigerator capable of reaching a base temperature of 4 K. We will use a low-T sample stick to cover the temperature range between 4 K and 298 K. To obtain a crystalline sample, rather than a glassy one, we will anneal the sample just below its melting point of 217 K.

4. Modes of Spectrometer and Data Reduction Details

We can use HFBS spectrometer in two different modes to extract the dynamical features of the sample under investigation. A detailed description of the spectrometer is given in Ref [ADGN03].

4.1. Fixed Window Scans

For reactor based neutron backscattering spectrometers, “Fixed window scans" or “elastic scans" are very powerful for getting a fast overview of the dynamics of a system and are often the starting point for quasi-elastic measurements. In this mode, we choose to count the neutrons with fixed initial and final wave vectors which results in analyzing neutrons scattered within a fixed energy window. To do so, we stop the moving monochromator (see below) and then change the external parameters like temperature and pressure and record the intensity. We can even assign a time scale to fixed window scans based on the instrumental resolution. In our case, assuming a FWHM of about 0.8 μeV, the slower limit would correspond to about 10 ns. Dynamic processes on a time scale slower than the instrumental resolution are not resolved

and thus are counted within the "elastic window". Faster motions of scattering particles can be resolved and will induce an energy loss or gain of the scattered neutrons, which then are no longer reflected by the analyzers to the detectors. One observes a decrease of the elastic window intensity as function of increasing temperature. Therefore, elastic or fixed window scans give a quick overview of the onset of motions faster than the time scale corresponding to the energy resolution (≈10 ns) and therefore, can be used to choose suitable temperatures for dynamic measurements.

4.2. Quasi-elastic Neutron Scattering

The HFBS spectrometer is configured in an inverse scattering geometry. This means that the energy of the neutron incident on the sample is varied while the final energy of the neutrons reaching the detectors is fixed.

A summary of the basic principle of operation of HFBS is outlined below (for more details on the instrument including a schematic see Appendix B and Ref[ADGN03]).

1. The “white" beam of neutrons produced by the reactor is velocity selected to yield neutrons that have energies around the desired energy of 2.08 meV. These neutrons are further focused in energy by a rotating phase space transform chopper and scattered towards the Doppler monochromator. The energy focused neutrons are backscattered from the Doppler monochromator thus selecting incident neutron energies, E_i, dependent upon the speed of the monochromator when reflected. While the Doppler is at rest, only neutrons with energies of 2.08 meV are backscattered from the monochromator. This is due to the lattice spacing of the Si hexagons that tile the surface of the monochromator.

2. The reflected neutrons from monochromator interact with the sample and are scattered from the sample with a distribution of energies.

3. Only neutrons with a particular scattered energy, E_f, reflect from the analyzer array into the detectors. Identical Si hexagons comprise the analyzer system, thus the backscattered neutrons all have energies of 2.08 meV. The energy transfer imparted on the sample is defined as $E = E_i - E_f$.

4. Neutrons scattered from the sample in a particular direction backscatter from particular analyzers and are counted one of the 16 detectors. This direction corresponds to the scattering angle, 2θ.

Question: What is the energy range of the neutrons incident on the sample, E_i?

Given the scattering angle 2θ and energy transfer E, we may calculate the magnitude of the momentum transfered to the sample Q. Kinematical arguments lead to the following relationship between 2θ, E, E_i, and Q:

$$\frac{\hbar^2 Q^2}{2m} = 2E_i - E - 2\sqrt{E_i(E_i - E)\cos(2\theta)}, \tag{4.1}$$

where m is the mass of the neutron.

The data acquisition system records the number of detector counts as a function of initial neutron velocity, v_i, where v_i is related to the instantaneous monochromator velocity, v_m, and the Bragg velocity of the neutrons with velocity 630 m/s, v_B, via $v_i = v_B + v_m$. The energy transfer to the sample, due to a Doppler shift of the neutron energies, is given by

$$E = 2E_B\left(\frac{v_m}{v_B}\right) + E_B\left(\frac{v_m}{v_B}\right)^2 \tag{4.2}$$

where E_B is the Bragg energy of neutrons with wavelength 6.27 Å, is written to the raw data file. This calculation is done using an encoded Doppler drive that provides information as to the acceleration as a function of position. The energy change is derived from this acceleration. Note that the motion of the monochromator is time-dependent, allowing the variation of E_i necessary to an inverse geometry spectrometer.

Question: Can you think of a way to change the incident neutron energies without moving the monochromator?

The raw data is recorded as $N(2\theta_j, E_k) = N_{j,k}$, the number of neutrons detected in detector j (at scattering angle corresponding to $2\theta_j$) with an energy transfer to sample of E_k. The quantity which reflects the dynamics of the scattering system most directly is $S(Q,E)$, the dynamic structure factor. What we measure, $N_{j,k}$, is closely related to the double differential scattering cross section $d^2\sigma/d\Omega dE$. This can be written in terms of various instrument-dependent parameters and the number of counts received in the detectors.

$$\left[\frac{d^2\sigma}{d\Omega dE}\right]_{j,k} = N_{j,k}\frac{A\eta(FC)}{N(FC)}\frac{\gamma_j}{\eta(E_f)}\frac{1}{\rho_N V}\frac{1}{\Delta\Omega_j}\frac{1}{\Delta E}. \tag{4.3}$$

Here,

- $\frac{A\eta(FC)}{N(FC)}$ is the *monitor normalization* of the incident beam area A times the beam monitor efficiency $\eta(FC)$ divided by the numebr of counts recieved by the beam monitor. 'FC' indicates the type of detector, a fission chamber.
- $\frac{\gamma_j}{\eta(E_f)}$ is the *vanadium normalization* of the detector intensity with the intensity scaling factor γ_j divided by the efficiency of the detector.
- ρ_N is the number density of scatterers in the sample.
- V is the volume of sample illuminated by the beam.
- $\Delta\Omega_j$ is the solid angle subtended by detector or analyzer angular coverage.

We obtain the dynamic structure factor $S(Q,E)$ using the first Born approximation (i.e. a single scattering event dominates the response of the sample).

$$S(Q,E) = \frac{4\pi}{\sigma}\frac{k_i}{k_f}\frac{d^2\sigma}{d\Omega dE}. \tag{4.4}$$

Here σ is the scattering cross section of the sample and $k_i(k_f)$ is the incident (final) neutron wavevector.

Note that for a sample in thermal equilibrium, the *detailed balance* condition is satisfied:

$$S(Q,-E) = e^{-E/k_B T} S(Q,E). \tag{4.5}$$

Here E is the sample energy gain. This condition is a technical way of saying that it is more likely that a sample will give energy to the neutron when the sample is at a high temperature as compared to when the sample is at a low temperature.

Question: Suppose that there is an excitation with an energy of 10 μeV. How large is the detailed balance effect at 4 K? How does this compare to a 10 meV excitation? (Hint: 1 meV = 11.6 K.)

5. Analysis and Interpretation of the Scattering Data

5.1. The Single Particle Model

We suppose that the methyl group may be treated as a rigid rotor undergoing rotations on a plane. If the rigid rotor has a moment of inertia I and an angular position ϕ, then the Hamiltonian operator H is:

$$H = -\frac{\hbar^2}{2I}\frac{\partial^2}{\partial\phi^2} + V(\phi). \tag{5.1}$$

For a methyl group, the rotational constant is $B = \hbar^2/2I = 654$ μeV. Suppose that the methyl group were completely free so that the hindering potential $V(\phi)$ were zero everywhere. Then, the (unnormalized) energy eigenstates would be $\psi_j(\phi) = e^{\pm ij\phi}$, with $E_j = Bj^2$, where $j = 0, \pm1, \pm2, \ldots$. To first approximation, the hindered rotors move through a three-fold potential with barrier V_3:

$$V(\phi) = \frac{V_3}{2}(1-\cos 3\theta) \tag{5.2}$$

The energy levels of the hindered rotor may be calculated by numerically diagonalizing the Hamiltonian H. This may be done using the DAVE software package[AKQ+09] and details of the calculation are given in Ref [Dim03].

Question: The librational energy levels may be obtained by applying the small-angle or harmonic approximation to $V(\phi)$. What is the spacing between the librational energy levels in terms of V_3 and I?

Figure 5.1 illustrates the rotational energy levels of the methyl group as a function of the barrier height V_3. Three cases may be distinguished. When the energy barrier is small, the rotational energy levels approach that of a free rotor $E_j = Bj^2$. In contrast, the energy levels approach the harmonic oscillator energy levels $E_n = (n_{\mathrm{lib}} + 1/2)\hbar\omega_{01}$ for large barrier strengths. Rotational tunneling is observable in a neutron backscattering experiment for intermediate strength barriers. Notice that the tunnel splitting is too small to be read directly on the energy scale in the figure.

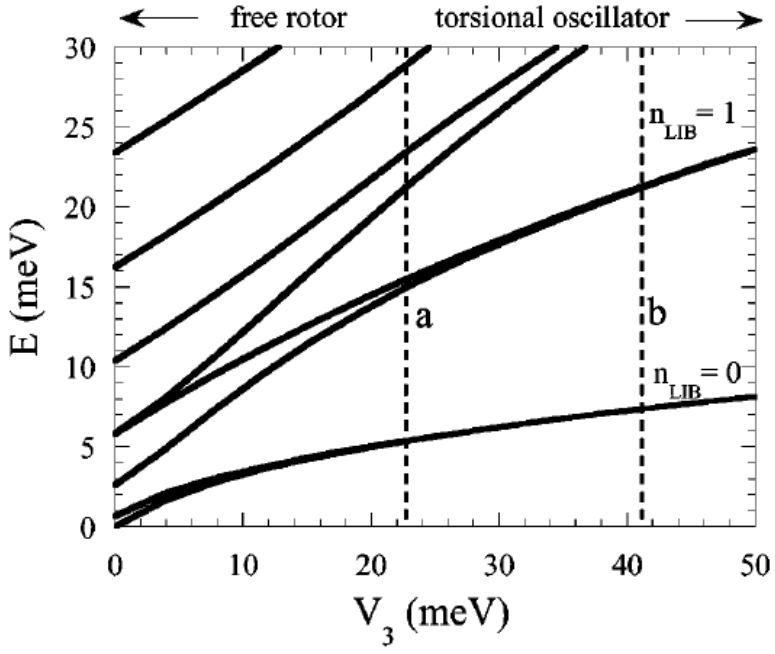

Figure 5.1: The energy levels of a hindered methyl rotor group as a function of barrier strength V_3[Dim03].

The tunnel splitting between the A and E levels for librational ground state, $n_{\text{lib}} = 0$, is shown as a function of barrier strength in Figure 5.2. As can be seen, the tunnel splitting $E_{\text{tunnel}} = \hbar\omega^0_{\text{tunnel}}$ depends exponentially strongly upon the strength of the potential barrier.

5.2. The Dynamic Structure Factor

One approach to analyzing the scattering data is to take advantage of the fact that the tunneling mode is dispersionless, i.e. the position, width, and shape of the tunneling peak is independent of Q. That is, we may sum over all of the detector groups to obtain $\overline{S}(E)$, the dynamic structure factor $S(Q,E)$ averaged over all measured Q. This will simplify the analysis and improve statistics at the expense of losing the geometric form factors of the motion.

At low temperatures, the total scattering law $\overline{S}(E)$ is a sum of elastic and inelastic components. If the sample were completely homogeneous, then the spacing between the A and E levels would be completely uniform throughout the sample and the transition energy would be sharply defined. In that case, the tunneling peaks would be represented by Dirac δ-functions:

$$\overline{S}(E) = \underbrace{A_0\delta(E)}_{\text{elastic}} + \underbrace{A_1\left(\delta(E+E_t)+\delta(E-E_t)\right)}_{\text{inelastic}} \tag{5.3}$$

The *elastic* scattering consists of a δ-function located at zero energy transfer. This contribution to the measured signal is to due to atoms which either do not move during the experimental time window or else return to their initial positions. The *inelastic* scattering consists of a pair of satellite peaks located at the tunneling energy $\pm E_t$.

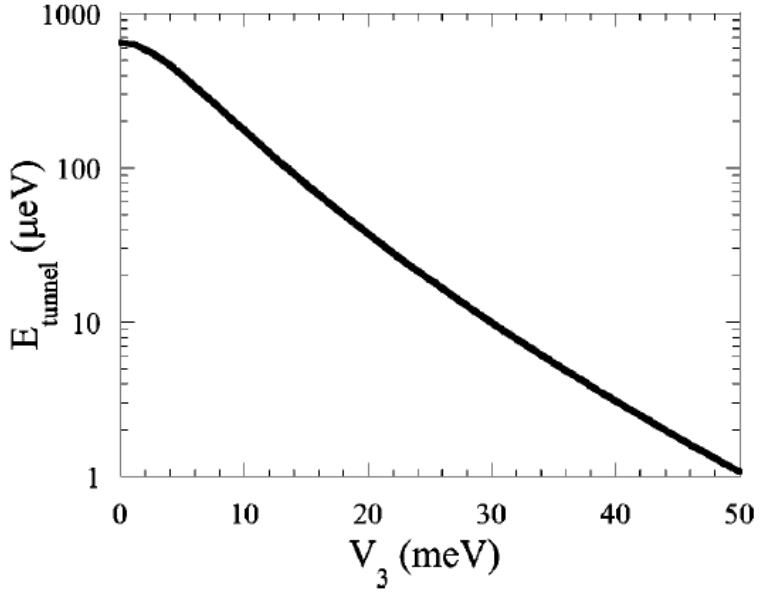

Figure 5.2: The tunneling energy E_{tunnel} is shown as a function of the barrier height V_3. [Dim03].

However, if there are variable perturbations throughout sample (e.g. lattice defects or impurities), then one may observe "inhomogeneous line broadening," i.e. an intrinsic linewidth at low temperatures. Neutrons probe the local dynamics and potential of hydrogenous systems, and so any disorder in the material may appear as a distribution of barrier strengths[DN00]. In that case, the tunneling peaks will appear as pair of Lorentzians located at $\pm E_t$ having a full width at half maximum Γ'.

$$\overline{S}(E) = \underbrace{A_0\delta(E)}_{\text{elastic}} + \underbrace{\frac{A_1}{\pi}\frac{(\Gamma'/2)^2}{(\Gamma'/2)^2+(E+\Delta)^2} + \frac{A_1}{\pi}\frac{(\Gamma'/2)^2}{(\Gamma'/2)^2+(E-\Delta)^2}}_{\text{inelastic}} \tag{5.4}$$

Question: Up to the resolution of your measurements, do the tunneling peaks in 4-fluorotoluene have an intrinsic linewidth at low temperature?

Question: Based upon the observed tunnel splitting Δ_0, what do you predict is the energy of librational mode E_{01}?

5.3. Temperature-dependence of the Scattering

The rotational dynamics of the methyl group as a function of temperature is an interesting example of a quantum-to-classical transition. At low temperature, one observes only the splitting of the ground state librational mode due to quantum-mechanical tunneling. As the

temperature increases, rotational tunneling is steadily replaced by rotational jump diffusion. Interaction of the methyl group with phonons may modulate the strength and the orientation of the effective orientational potential. In most, but not all, systems, coupling between phonons and methyl groups leads to a softening and a broadening of the tunneling peak. Quasi-elastic broadening may also appear as thermal fluctuations lift the degeneracy of the two separate E levels. As the temperature increases still further, one observes only quasi-elastic broadening corresponding to classical, rotational jump diffusion.

At 'intermediate' temperatures where both quasi-elastic and inelastic neutron scattering may be observed, the scattering law $\overline{S}(E)$ is:

$$\overline{S}(E) = \underbrace{A_0\delta(E)}_{\text{elastic}} + \underbrace{\frac{A_2}{\pi}\frac{(\Gamma/2)^2}{(\Gamma/2)^2+E^2}}_{\text{quasi-elastic}} + \underbrace{\frac{A_1}{\pi}\frac{(\Gamma'/2)^2}{(\Gamma'/2)^2+(E+\Delta)^2} + \frac{A_1}{\pi}\frac{(\Gamma'/2)^2}{(\Gamma'/2)^2+(E-\Delta)^2}}_{\text{inelastic}} \tag{5.5}$$

Finally, at high temperatures, the scattering is dominated by stochastic reorientation or rotational jump diffusion:

$$\overline{S}(E) = \underbrace{A_0\delta(E)}_{\text{elastic}} + \underbrace{\frac{A_2}{\pi}\frac{(\Gamma/2)^2}{(\Gamma/2)^2+E^2}}_{\text{quasi-elastic}} \tag{5.6}$$

In many systems, the softening and broadening of the tunneling peak obeys a simple Arrhenius law:

$$\Delta E_t(T) \quad \propto \quad \exp\left(-\frac{E_S}{k_B T}\right) \tag{5.7}$$

$$\Gamma(T) \quad \propto \quad \exp\left(-\frac{E_\Gamma}{k_B T}\right) \tag{5.8}$$

The activation energies E_S and E_Γ are generally attributed to the phonon density of states[PH97]. Since the shift of the tunnel peak depends upon all states where the methyl group is coupled to by lattice excitations, E_S is less than the the librational mode spacing E_{01}. On the other hand, the activation energy E_Γ is approximately equal to the spacing of the librational mode E_{01}.

Question: Do the observed positions and widths of the tunneling peak in 4-fluorotoluene obey an Arrhenius law? If so, how do the activation energies E_S and E_Γ compare to the librational excitation energy E_{01}?

A. Effects of the Sample Geometry on Self Shielding and Multiple Scattering

One must consider a number of issues when determining appropriate sample geometry. A naïve philosophy in designing sample geometry is to make the sample as big as possible in order to obtain as many scattering events in the shortest possible time. Unfortunately, optimization of the experiment is not as simple as this. Sample design involves careful consideration of the composition of the sample in terms of its scattering and absorption cross sections.

In an inverse geometry spectrometer like HFBS where the beam passes through the sample twice one must consider *self-shielding* effects which reduce the intensity recieved at the detectors *via* absorption. In general, absorption in the sample is proportional to the neutron wavelength. On a backscattering spectrometer using Si(111), $E_f = 2.08$ meV and $\lambda = 6.27$ Å, resulting in the cross section for absorption being 3.5 times larger than for thermal neutrons where the wavelength is 1.8 Å.

In order to understand the extent to which you have to correct for multiple scattering/self-shielding, it is important to know how strong a scatterer/absorber your sample is. The transmission in the forward direction ($2\theta = 0$) is often calculated and expressed in terms of a percentage of the incident beam that is scattered/absorbed. Suppose that the sample has a microscopic bound scattering cross section $\sigma_{tot} = \sigma_{inc} + \sigma_{coh}$ and microscopic absorption cross section σ_{abs}. Then, the macroscopic scattering Σ_S and absorption Σ_A cross sections (in units of cm^{-1}) are given by:

$$\Sigma_S = \sigma_{tot}\rho \tag{A.1}$$

$$\Sigma_A = \sigma_{abs}\rho, \tag{A.2}$$

where ρ is the molar density of the atoms. For a flat plate sample of thickness t at an angle ϕ to the incident beam, scattering and absorption is:

$$\text{scattering} = 1 - \exp\left[1 - \Sigma_S t \sec\phi\right] \tag{A.3}$$

$$\text{absorption} = 1 - \exp\left[1 - \Sigma_A t \sec\phi\right] \tag{A.4}$$

For a thin annular sample cell,

$$\text{scattering} = 1 - \exp\left[1 - \pi\Sigma_S t\right] \tag{A.5}$$

$$\text{absorption} = 1 - \exp\left[1 - \pi\Sigma_A t\right] \tag{A.6}$$

These are good approximations when $\exp[1 - \pi\Sigma t] > 80\%$.

We illustrate the self-shielding corrections for a vanadium sample in the flat plate and annular geometries, where $\sigma_{tot} = 5.10$ barns and $\sigma_{abs} = 5.08$ barn for 1.8 Å neutrons. The intensity in the detectors is very sensitive to the thickness t of the sample as well as its geometry. If we assume these two geometries for the same amount of scattering (5%, 10%, and 20% scatterers) and assume that the samples are completely illuminated by the incident beam, then we obtain the results shown in Figure A.1. The corrected intensity is obtained using $I_{corr}(2\theta, E) = I_{obs}(2\theta, E)/A_{ssc}$, where $I_{obs}(2\theta, E)$ is the observed intensity. It is quite clear that there is a much stronger angle dependence for the correction factor of the slab geometry whereas the corrections are much less for the annular cell. Furthermore, an evaluation of the correction factor is impossible near the orientation angle, 130° in the present example, for the slab geometry. Therefore, it is advantageous to use an annular geometry for backscattering. Note that because the beam goes through the sample twice on HFBS, the sample transmission due to the presence of absorption must be *squared*.

When one increases the thickness of the sample for a system with medium absorption cross section, the intensity will not significantly increase but the effects of multiple scattering will

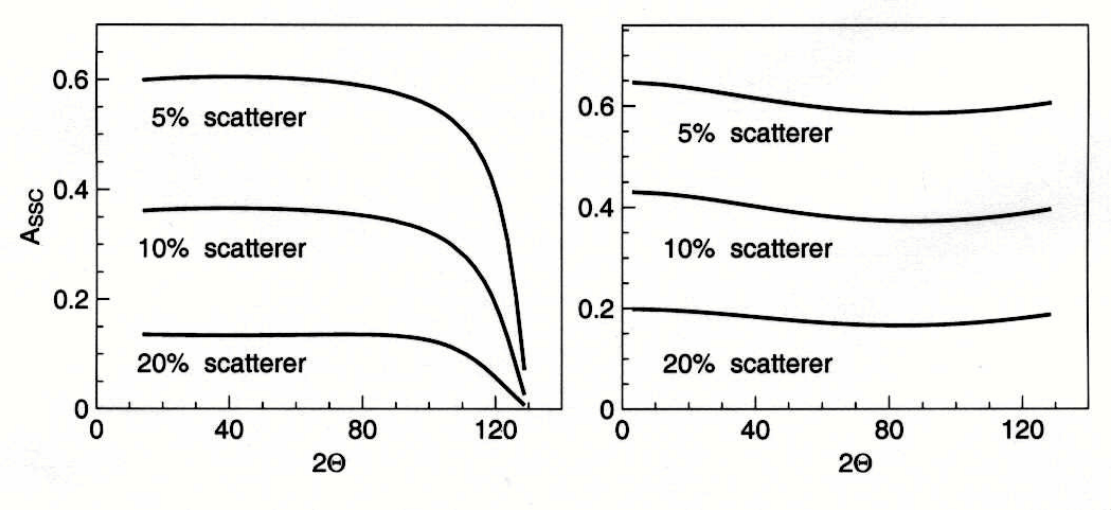

Figure A.1: The self-shielding factor as a function of scattering angle 2θ are compared: flat plate oriented at 130° to the incident beam (left) and a thin annulus.

certainly be enhanced. Corrections for multiple scattering are not trivial and, for many systems in which the scattering function is not known *a priori*, may not be possible at all.

Figure A.2 illustrates the effects that multiple scattering can have on a system, in this case viscous glycerol. This sample was measured on the IN10 backscattering spectrometer at the ILL where structural relaxation (viscous flow) is on the time scale of tenths of nanoseconds. There is clear broadening of the lineshape with increasing Q due to the dynamics of the system. However, at $Q = 0.19$ Å^{-1}, structural relaxation cannot be resolved because it is too slow at this small Q. The apparent broadening in the wings is entirely due to multiple scattering.

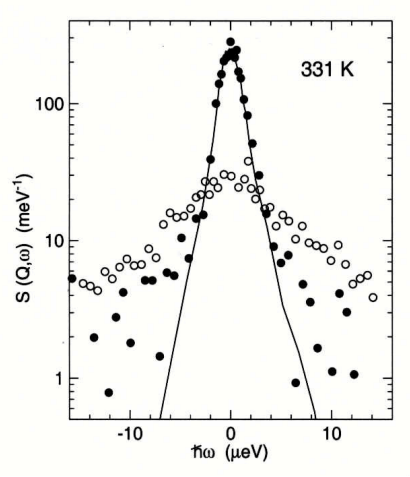

Figure A.2: Scattering intensity of viscous glycerol taken on the IN10 backscattering instrument illustrating the effects of multiple scattering on $S(Q,E)$[WCR+96] . Solid line represents the instrumental resolution, open symbol are data taken at $Q = 1.4\,\text{Å}^{-1}$ and the closed symbols are data taken at $Q = 0.19\,\text{Å}^{-1}$.

B. Instrument Characteristics for the High Flux Backscattering Spectrometer

- Website: `http://www.ncnr.nist.gov/instrument/hfbs`
- Si (111) analyzers cover 20% of 4π steradians.
- $\lambda = 6.27$ Å
- $E_f = 2.08$ meV
- $v_n = 630$ m/s
- 16 ^{3}He detectors covering $14° \leq 2\theta \leq 121°$
- Dynamic range: $0.25\,\text{Å}^{-1} \leq Q \leq 1.75\,\text{Å}^{-1}$; $-36\,\mu\text{eV} \leq E \leq +36\,\mu\text{eV}$.
- Instrumental resolution: $\delta Q = 0.1\,\text{Å}^{-1} - 0.2\,\text{Å}^{-1}$; $\delta E \leq 1\,\mu\text{eV}$
- Flux at sample: $\Phi \approx 1.4 \times 10^5 \text{n/cm}^2\text{/s}$
- Beam Size at Sample: 2.8 cm by 2.8 cm.
- Signal-to-noise: 400:1 for vanadium foil (10% scatterer).
- Standard sample environments: Closed cycle refrigerator (5 K to 325 K); Closed cycle refrigerator (50 K to 600 K); Orange cryostat (1.5 K to 300 K).

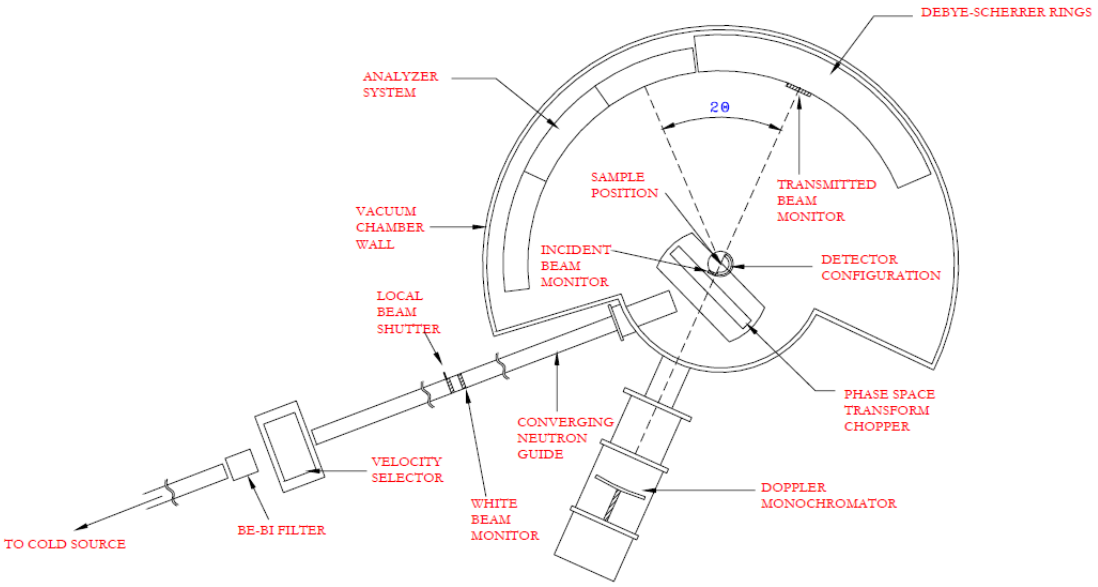

Figure B.1: Schematic of the High Flux Backscattering Spectrometer[ADGN03].

C. Instrumental Resolution

In an experiment with an ideal instrument, we could measure the sample's scattering response directly. However, real neutron spectrometers (or any measurement apparatus) have finite resolution which distorts the measured distribution. The origin of the resolution distortion is due to many instrument-specific factors which lead to an accumulation of (hopefully small!) uncertainties. These uncertainties have the general effect of *blurring* the overall response. The effects of instrumental resolution often can be quantified in the instrumental resolution function $R(Q,E)$. Mathematically, the resolution function and the intrinsic scattering function are convoluted to yield the measured response. We present here an example of a convolution of two functions and the effects of the resolution width.

In this example, we assume that the resolution function, $R(E)$, is a normalized Gaussian centered at zero:

$$R(E) = \frac{1}{\sqrt{2\pi\sigma^2}} e^{-\frac{E^2}{2\sigma^2}}. \tag{C.1}$$

The intrinsic scattering function $S(E)$ is a triangle function centered at zero with base Δ one unit wide ($\Delta = 1$) and unit height.

$$S(E) = \frac{2}{\Delta}\left[\left(E+\frac{\Delta}{2}\right)\Theta\left(E+\frac{\Delta}{2}\right) - 2E\Theta(E) + \left(E-\frac{\Delta}{2}\right)\Theta\left(E-\frac{\Delta}{2}\right)\right], \tag{C.2}$$

where Θ is the unit step function.

The measured response $I(E)$ is given by the convolution integral:

$$I(E) = S(E) \otimes R(E) = \int_{-\infty}^{+\infty} dE' S(E') R(E - E'). \tag{C.3}$$

When the Gaussian width σ is small, the Gaussian approaches a Dirac δ-function, and the resolution of the convolution looks very similar to the original triangle function. Figure C.1 shows this result for a full-width at half-maximum (FWHM is approximately 2.3458σ) of 0.01. When the width is larger, the resulting convolution product looks more distorted and blurred. Figure C.2 shows such a case when the resolution width is 0.5.

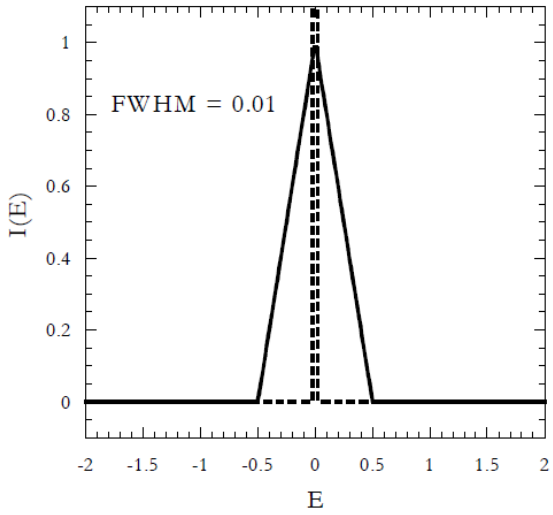

Figure C.1: Result of the convolution of the triangle function with a Gaussian of width 0.01.

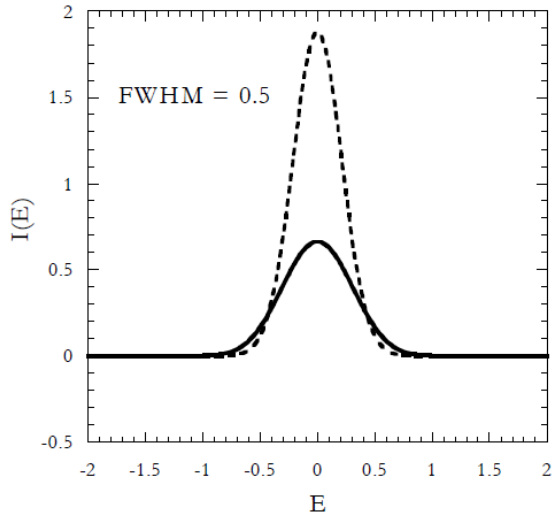

Figure C.2: Result of convolution of the triangle function with a Gaussian of width 0.5.

Note that as $R(E)$ becomes more narrow, the convolution product looks more like $S(E)$. For infinitely sharp resolution, $R(E) = \delta(E)$, the convolution product is *exactly* $S(E)$. Knowledge of the instrumental resolution function is essential for detailed lineshape analysis. Often this can be measured using an elastic scatterer.

In many cases, the instrumental resolution can be measured directly and used in the model fitting procedure *via* the convolution product. If we measure the scattering function from a purely elastic scatterer (ignoring the angular or Q-dependence for now) then the measured quantity is directly proportional to the resolution function. In particular, the elastic scattering function can be represented by a Dirac δ-function with area A: $S_{EL}(E) = A\delta(E)$. When convoluted with the resolution function, we get the measured response:

$$I_{\text{measured}}(E) = A \times \delta(E) \otimes R(E) = A \times R(E). \tag{C.4}$$

Not that we must normalize the resolution function so that it has unit area. This is necessary so that we can extract the integrated intensity of the intrinsic lineshape $S(E)$ from the fit to the model. Since the integrated intensity of the convolution product of two functions is equal to the product of the areas of the two functions, then, if one of these areas in unity, then the other must be the total area of the measured intensity.

REFERENCES

[ADGN03] Meyer A., R. M. Dimeo, P. M. Gehring, and D. A. Neumann. *Rev. Sci. Instrum.*, 74:2759, 2003.

[AKQ+09] R. T. Azuah, L. R. Kneller, Y. Qiu, P. L. W. Tregenna-Piggott, C. M. Brown, J. R. D. Copley, and R. M. Dimeo. *J. Res. Natl. Inst. Stan. Technol.*, 114:341, 2009.

[CL15] J. M. Carpenter and C. K. Loong. *Elements of Slow-Neutron Scattering*. Cambridge University Press, 2015.

[Dim03] R. M. Dimeo. *Am. J. Phys.*, 71:885–893, 2003.

[DN00] R. M. Dimeo and D. A. Neumann. *Phys. Rev. B*, 63:014301, 2000.

[PH97] M. Prager and A. Heidemann. *Chem. Rev.*, 97:2933–2966, 1997.

[PHLMw90] M. Prager, R. Hempelmann, H. Langen, and W. Müller-warmuth. *J. Phys.: Condens. Matter*, 2:8625–8638, 1990.

[Pre81] W. Press. *Single-Particle Rotations in Molecular Crystals*. Springer, 1981.

[SMT+62] D. W. Scott, J. F. Messerly, S. S. Todd, I. A. Hossenlopp, D. R. Douslin, and J. P. McCullough. *J. Chem. Phys.*, 37:867–873, 1962.

[WCR+96] J. Wuttke, I. Chang, O. G. Randl, F. Fujara, and W. Petry. *Phys. Rev. E*, 54:5364, 1996.